In-plane Thermoelectric Properties of MXene and poly(3,4-ethylenedioxythiophene)/poly 4-styrenesulfonate (PEDOT/PSS) Hybrid Films

Takao Ishida*, Mihoko Motoki, Atsushi Yamamoto,

Kazuki Imasato, Masanobu Miyata and Michihiro Ohta

Global Zero Emission Research Center, National Institute of Advanced Industrial Science and Technology (AIST), Tsukuba, Ibaraki 305-8569, Japan.

ORCID

Takao Ishida: 0000-0001-8662-1163

Atsushi Yamamoto: 0000-0002-9210-2682

Kazuki Imasato: 0000-0001-7294-1780

Masanobu Miyata: 0000-0002-1290-0984

Michihiro Ohta: 0000-0002-9093-7117

Corresponding author

t-ishida@aist.go.jp （TI）

Abstract

We investigated the in-plane thermoelectric properties of hybrid films composed of Ti_3C_2-MXene and poly(3,4-ethylenedioxythiophene)/poly-4-styrene sulfonate (PEDOT/PSS). The Seebeck coefficient increased as the amount of cleaved MXene in the PEDOT/PSS matrix increased, and the power factor (*PF*) reached its maximum at a 5% MXene ratio. Furthermore, dimethyl sulfoxide (DMSO) rinse improved the electrical conductivities of the films, and then, a higher *PF* of 86.8 μW/mK^2 was obtained. We evaluated the in-plane thermal conductivities of these hybrid films, to estimate in-plane figure of merit (*zT*). The highest in-plane *zT* of the films was 0.019, and this value is twice that of PEDOT/PSS film without MXene.

1. Introduction

A great deal of research on organic polymer thermoelectric (TE) materials has been undertaken in the last 15 years. Of the many kinds of organic materials, poly(3,4-ethylenedioxythiophene)/poly-4-styrene sulfonate (PEDOT/PSS)[1-8] films have attracted particular attention. In practice, many nanomaterials have been mixed with PEDOT/PSS to increase the power factor (*PF*), which can be expressed as $PF=S^2\sigma$, (where S and σ are the Seebeck coefficient and electrical conductivity, respectively) either by increasing the conductivity or by increasing the Seebeck coefficient These materials include gold nanoparticles[9], Bi_2Te_3 nanoparticles[10], Te nanowires[11], and single wall carbon nanotube (SWCNT)[12-14].

Recently, MXene has often been reported as a new material for mixing with PEDOT/PSS.[15,16] Among the very many kinds of MXenes, Ti-based MXene (Ti_3C_2) is already commercially available, has good affinity with PEDOT/PSS and is soluble in hydrophilic solvents.[17] It has been reported that Ti-based MXene itself has very high electrical conductivity.[18,19] Furthermore, a hybrid film comprising PEDOT/PSS and MXene is also expected to be used for other applications including as an electrode for electrochemical devices,[20] and as electromagnetic interference shielding material[21].

For TE applications, first, Guan *et al.* reported the high TE properties of Ti-based

MXene and PEDOT/PSS hybrid films.[15] Moreover, since MXene is not sold in single layers, it is necessary to separate the layers. For example, Park *et al.* mixed Ti-based MXene with PEDOT/PSS by using ball-milling to reduce its size before mixing, and showed that as MXene decreases in size, the *PF* value increases.[16] Park *et al.*, also concluded the reason for the increase in the Seebeck coefficient compared with that of undoped PEDOT/PSS film is due to the energy filtering effect (Fig. 1a).[16] It is understood that when an energy filtering effect occurs, a suitable barrier is formed for carrier transfer at around 0.1 eV between the doped nanomaterial and the conductive polymer part. The Seebeck coefficient increases because the low-energy barrier prevents the transfer of the low-energy carriers.[22-24]

Another problem as regards organic TE materials is the calculation of the dimensionless performance index (figure of merit) zT, which can be written as $zT = S^2\sigma T/k$, where T and k are the absolute temperature and thermal conductivity, respectively. Typically, the Seebeck coefficient and conductivity are measured in-plane (Fig. 1b), while to date the through-plane thermal conductivity has been used to evaluate the zT of organic TE materials, by assuming that there is neither anisotropy in the structure nor electrical conductivity (Fig. 1c).[2,3,5,7] One reason for using the through-plane thermal conductivity was that it was particularly difficult to measure the in-plane thermal conductivity of thin

films.

In the hybrid PEDOT/MXene system, the MXene flakes are thought to be distributed in the film in a direction parallel to the surface (Fig. 1a), and it is predicted that the thermal conductivity in the through-plane and in-plane directions of the film will differ greatly. In addition, since the in-plane power generation capacity is expected to be utilized when the film is fabricated into a TE device,[25-27] it is very important to measure the in-plane *zT*.

Moreover, in terms of thermal applications other than thermoelectricity for MXene-polymer hybrid films, it is necessary to collect thermal conductivity measurement data. In particular, the reported thermal conductivity of MXene/polymer composite films varied widely, from 0.5 W/mK[28] to 50 W/mK.[29] Since the past reported values vary so greatly, it is necessary to carefully examine the relationship between the amount of doped MXene and thermal conductivity even in other heat-related applications.

Several techniques for measuring the in-plane thermal conductivity of thin films can be used to accurately measure in-plane *zT*. With PEDOT/PSS, at least two groups have reported the in-plane *zT* value by devising a method to measure the in-plane thermal conductivity.[30,31] One technique is the 3-omega method.[30] In this case, the in-plane *zT* of PEDOT/PSS film is estimated to be about 0.1, namely about one-fifth of the value for previous cases using through-plane thermal conductivity, with a maximum *zT* of 0.42.[3]

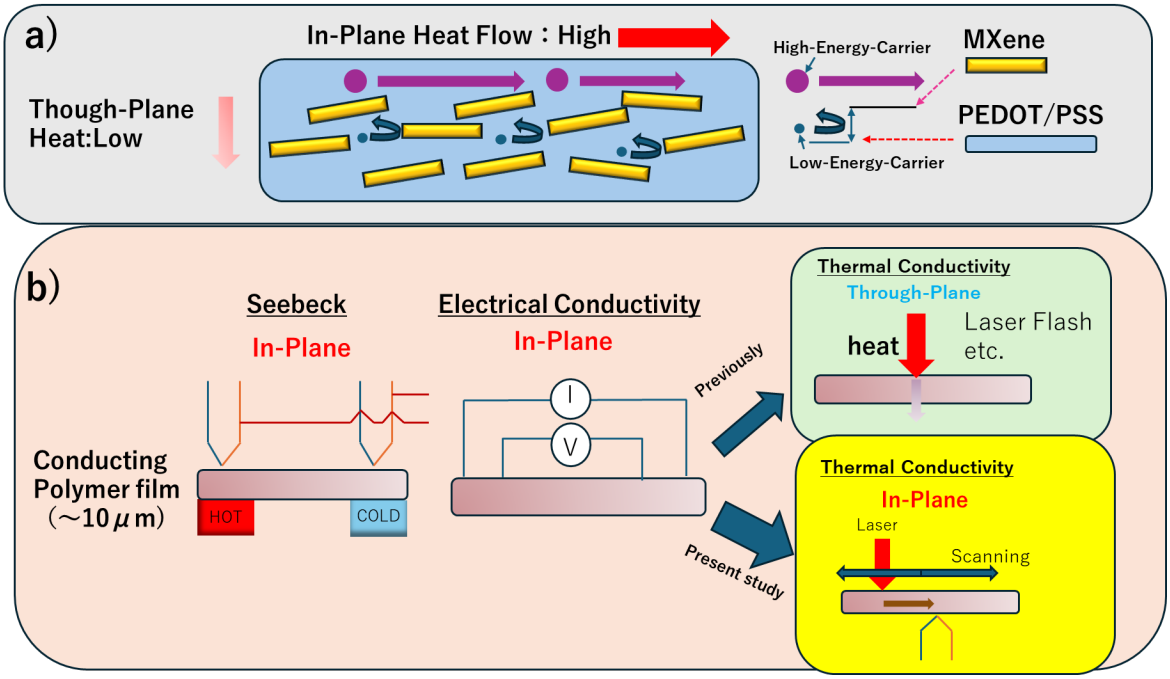

Fig. 1 a) Schematic of MXene and PEDOT/PSS hybrid films. According to previous papers[16] when flakes of MXene are mixed with PEDOT/PSS, an energy barrier is generated between MXene and PEDOT/PSS, increasing the Seebeck coefficient, because it prevents the movement of carriers with low kinetic energy; b) Schematic of thermoelectric measurements; Seebeck-coefficient; electrical conduction using a 4-point probe, through-plane thermal conductivity and in-plane thermal conductivity(diffusivity) method. In this case, we measure the thermal diffusivity of sheet materials in the in-plane direction by scanning with a laser heating AC method.

There is another method with which to estimate the in-plane thermal conductivity of thin films is measuring the through- plane thermal diffusivity of a multilayer film tilted at 90 deg.[31] On the other hand, the in-plane thermal diffusivities can also be measured by scanning with laser heating AC method (Angstrom method Fig. 1b).[32] We used it because this technique is easy to apply to organic thin film.

In this study, we estimated the in-plane TE properties of cleaved Ti-based MXene/PEDOT/PSS hybrid films. We measured the work functions of these hybrid films, to evaluate the effective energy barrier and thus increase the Seebeck coefficient. The thermal diffusivity, specific heat and density of the hybrid films were measured with different mixing ratios of MXene and PEDOT/PSS, and then we estimated the in-plane thermal conductivity. Using in-plane thermal conductivity, the in-plane zTs of MXene/PEDOT/PSS hybrid films were calculated.

2. Experimental

The PEDOT/PSS water dispersion (PH1000) and Ti-C MXene were purchased from Clevios and Japan Material Technologies Corp., respectively. First, Ti-C MXene was dispersed in dimethyl sulfoxide (DMSO) at a concentration of 10 mg/ml. To make MXene as fine as possible, a cleaving process was performed with an ultrasonic homogenizer

(Mitsui Electric Seiki, UX-50) at an output power of 25 W. To form mixed films, the diluted MXene DMSO solution was mixed with PEDOT/PSS solution at volume ratios of 2%, 5%,10% and 20%. The mixed solution was further stirred for 1 h at room temperature.

The films were prepared by the drop casting method. The solution was drop-cast onto a glass substrate or a PDMS polymer and dried at 90 °C for 10 min, followed by annealing at 130 °C for 10 min. For some samples, to further improve the film properties, the films were rinsed with pure DMSO twice to remove any PSS remaining in the PEDOT/PSS parts. After the films were washed with DMSO, they were annealed again at 130 °C for 10 min, and then washed 3 times with pure water. The film thickness was in the 5~10 μm range. We also made hybrid films with ratios of 30% and 50%, but these were too fragile to be properly evaluated. To measure thermal diffusivity, we made a free-standing film, which was formed on the PDMS surface.

The surface morphology was measured using a scanning electron microscope (TM3030 miniscope, Hitachi Hightech). The film thickness was measured with a surface roughness meter (SE500A, Kosaka Laboratory, Ltd.). The electrical conductivity of the film on a glass substrate was measured using a Nittoseiko Analytech Loresta GXII, and the Seebeck coefficient was determined with a home-made setup that employed R-type thermocouples.

The Seebeck coefficient measurements were made at less than 65% humidity, because the Seebeck coefficient increases when the humidity exceeds 80%.[4,5] We undertook the measurement by bringing the thermocouple into direct contact with the material. The work function values of films, which are related to the Seebeck coefficients, were measured with an atmospheric work function meter (RIKEN KEIKI Co. AC-2).

The thermal conductivity (κ) was calculated from the thermal diffusivity (α), specific heat (Cp), and density (ρ) using the equation: $\kappa = \alpha \times C_p \times \rho$. The in-plane and out-of-plane thermal diffusivities were measured with a LazerPit (Advanced Riko) and an aiPhase thermal diffusivity meter (aiPhase mobile), respectively. The C_p of the free-standing films was measured with a differential scanning calorimeter (DSC, NETZSCH DSC 3500). The density of each film was calculated by using the volume and mass of a free-standing film formed on the PDMS surface.

3. Results and Discussion

3-1. Film characterization

Before mixing PEDOT/PSS with MXene, we used an ultrasonic vibration homogenizer to cleave the MXene. Figs.2a-2c show the structural change in MXene with cleaving time as observed by SEM. Figs.2d-2e show histograms of the size of these MXene flakes with

cleaving time. After 8 h and 13 h of homogenization, the MXene became smaller, and after 8 h, the MXene was sufficiently cleaved into a monolayer as shown in the histograms. Fig. S1 shows the change in the Seebeck coefficient of the MXene/PEDOT/PSS film mixed with a 20% ratio of MXene. The Seebeck coefficient was successfully increased by increasing the cleaving time. We also made hybrid films with 30% and 50% MXene ratios, but, unfortunately, the films were easily broken by DMSO and pure water rinsing, so in the present study we evaluated hybrid films with up to a 20% MXene ratio.

Hereafter, we compare hybrid films that use 13h-cleaved MXene and film that contains uncleaved MXene. Fig. 3 shows SEM-EDX data for PEDOT/PSS hybrid films with 13h-cleaved MXene. The top view SEM observation clearly shows that the number of protrusions on the film surface increases according to the amount of incorporated MXene (cf. Figs 3a-3e). The elemental ratios as measured by EDX using top view SEM images are shown in Table S1. Ti increases in proportion to the amount of incorporated MXene. The Ti EDX image of the 10% MXene mixed film in Fig. 3c (Fig. 3f) shows that the Ti contrast is stronger in the film-like protrusions. The large white foil in the 10% cross-sectional image shown in Fig. 3f also corresponded to the Ti rich region. These data show that MXene is incorporated in response to the preparation value, and a reasonable amount of MXene is dispersed in the PEDOT/PSS matrix. In addition, we observed that the

MXene flakes were aligned parallel to each other

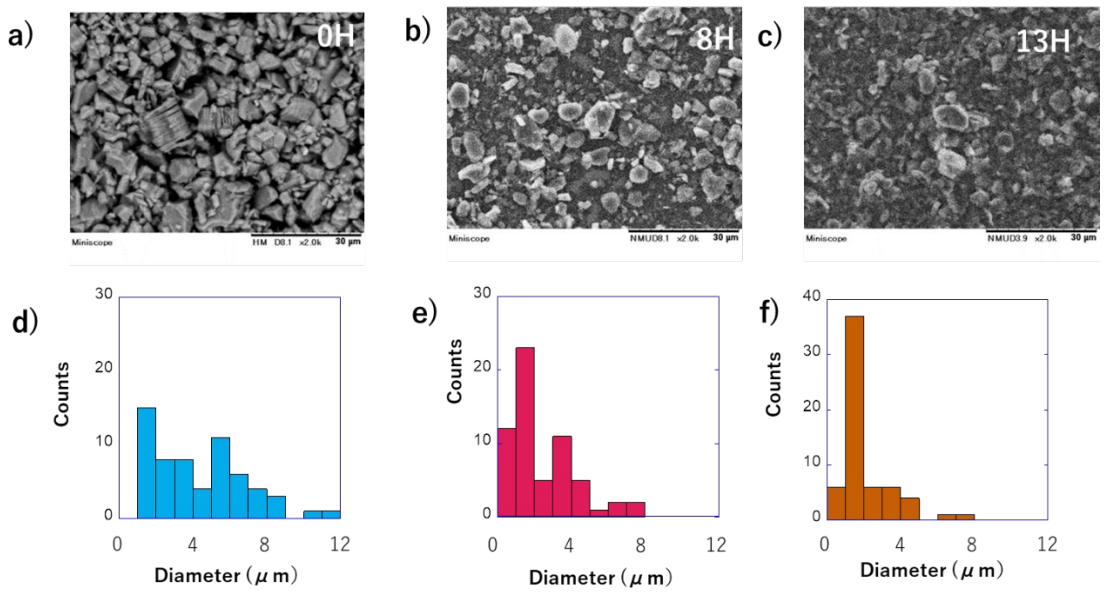

Fig. 2 SEM images of Ti-based MXene treated with an ultrasonic homogenizer (a) 0h; (b) 8h; and (c) 13h. Histograms of size of these MXene flakes. (d) 0h; (e) 8h; and (f) 13h.

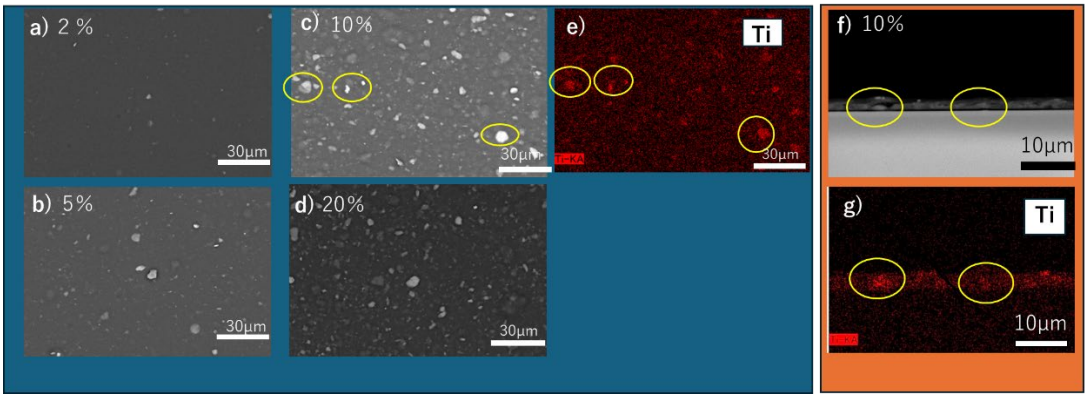

Fig. 3 SEM images (Top view) of MXene(13h) /PEDOT/PSS films: (a) 2%;(b) 5%;(c) 10% and ;(d) 20%. (e) Cross-sectional SEM image of 10% film;(f) EDX image of Ti of (c); (g) EDX image of Ti of (f).

to the surface. For the hybrid films with un-cleaved MXene, an image of the large clumps of MXene was obtained as it was (Fig. S1). The EDX data for the film containing un-cleaved MXene (Table S2) were not as high as expected for Ti in 10% of the samples compared with those with cleavage. In several measurement data, Ti was low in only 10% of the samples. Since the amount of Ti increased to a certain extent at a 20% ratio, it appears that it is not difficult to mix un-cleaved MXene into the PEDOT/PSS matrix. Thus, we consider that the lower amount of Ti may be due to the EDX resolution.

3-2. TE properties of hybrid films (Seebeck coefficient, electrical conductivity and power factor)

Below, we discuss the differences between the TE properties of film doped with cleaved MXene and film doped with un-cleaved MXene. Fig. 4 shows the detailed TE properties of thin films of MXene/PEDOT/PSS. The characteristics of PEDOT/PSS with cleaved MXene are shown in Figs. 4a-4c. For comparison, the TE properties of PEDOT/PSS films with un-cleaved MXene are shown in Figs.4d-4f. Figs.4a and 4d show the change in the Seebeck coefficient as a function of the MXene ratio. For the hybrid films with cleaved MXene, the average Seebeck coefficients (blue circles in Fig. 4a)

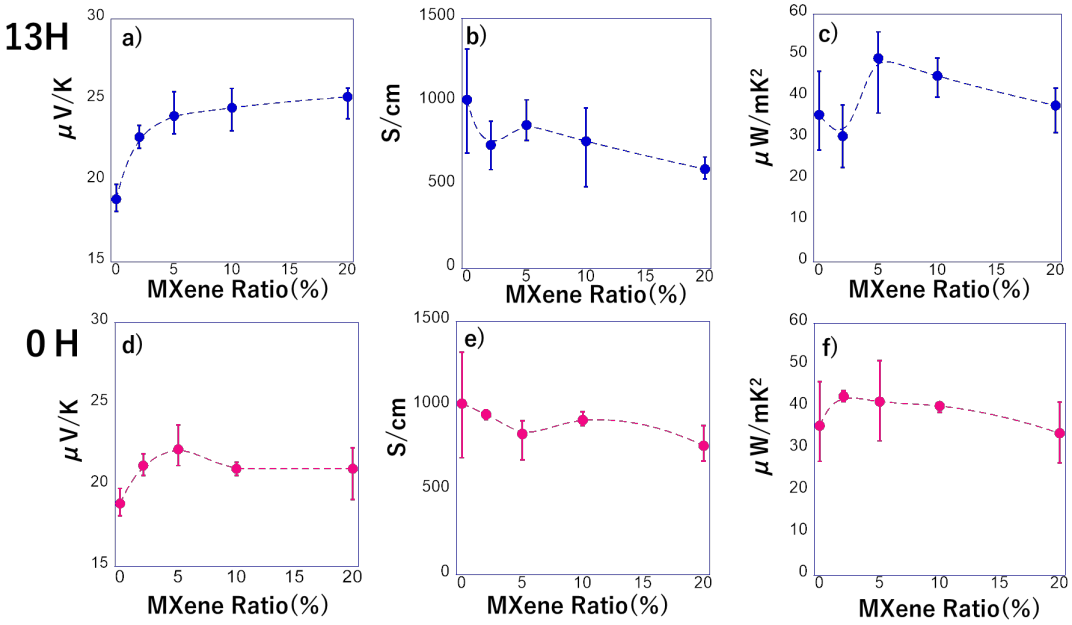

Fig. 4 TE properties of Ti-based MXene/PEDOT/PSS hybrid films with different MXene ratios at room temperature (about 298K): (a) Seebeck coefficients; (b) electrical conduction; and (c) power factors of hybrid films mixed with cleaved MXene. (d) Seebeck coefficients; (e) electrical conduction; and (f) power factors of hybrid films mixed with un-cleaved MXene. In the figures, the average value for three or more samples is indicated by a circle, the upper limit of the bar is the maximum value, and the lower limit is the minimum value.

increased by about 7 μV/K up to a 20% ratio compared with that of the PEDOT/PSS (denoted 0%) film. Figs.4b and 4e show the electrical conductivities for the hybrid films as a function of the MXene ratios. The electrical conductivities of the hybrid films with

Sample type	Seebeck coefficients (μ V/K)	Electrical conductivities (S/cm)	Max*PF* (μW/mK^2)
PEDOT/PSS	19.8	1317	46.1
Rinsed 13h 2%	23.9	1262	72.1
Rinsed 13h 5%	26.8	1209	86.8
Rinsed 13h 10%	26.4	611	57.7
Rinsed 13h 20%	26.5	504	42.6

Table 1. Summary of maximum TE data of DMSO-rinsed 13h-cleaved MXene/PEDOT/PSS hybrid films.

cleaved MXene further decreased when the ratio exceeded 10%. We consider that the electrical conductivity is reduced by the fine and uniform dispersion of the mixed MXene in the case of the hybrid films with cleaved MXene. On the other hand, for hybrid films with un-cleaved MXene, MXene chunks that are close to bulk, do not interfere with the conductive path of the carriers in the film, so the decrease in electrical conductivity is thought to be small. Figs. 4c and 4f show the dependence of the *PF* of the hybrid films on the MXene ratios. The average *PF* values are also greater in hybrid films with cleaved MXene than those of hybrid films with un-cleaved MXene. In some samples of the hybrid films with cleaved MXene, DMSO rinsing was performed twice more to further improve

the conductivity. The Seebeck coefficient and conductivity increased with this process, and the maximum values were obtained under all conditions. The maximum values for each ratio are shown in Table 1. At a ratio of 5%, we obtained a maximum *PF* of 86.8 $\mu W/mK^2$, which is the highest value achieved in our experiments.

The trend of our TE data is likely to be similar to the results reported by Park *et al.*, using ball milling to reduce the size of MXene.[16] Park *et al.*, concluded that the increase in the Seebeck coefficient is due to the creation of an effective energy barrier between the PEDOT part and MXene.[16] There is considerable debate about the theory and analysis of energy filtering effects in organic/inorganic hybrid TE materials,[22-24] and there is no consensus at this stage. However, it is necessary to evaluate whether an energy filtering effect is occurring. If the particles or flakes mixed into the polymer matrix are sufficiently small, it is thought that the difference in work function between MXene and polymer film will be useful with respect to discussing the change in Seebeck coefficients of the thin film.[15,16] For example, Park *et al.*, found that the Seebeck coefficient value by further tetrakis(dimethylamino)ethylene(TDAE) processing is maximized when the work function difference between hybrid film and MXene has a minimum value of 0.14 eV.[16] To be exact, it is thought that the Seebeck coefficient can be effectively increased by energy filtering effects if the barrier height is below 0.2 eV[33]

We used their method to examine the relationship between the amount of MXene doping and the change in the Seebeck coefficient as a result of the energy filtering effect. We measured the work functions of hybrid films with cleaved MXene in air. The work function decreases as the amount of MXene increases except with 2% ratio samples (Fig. 5a). We have plotted the difference between the work function value of Ti-based MXene (reliable value, approximately 4.7 eV)[34-36] and the measured work function value, as well as the change in the Seebeck coefficient (Fig. 5b). As the effective barrier height decreases, the Seebeck coefficient increases. Since the degree of change is very similar, the behavior of the effective barrier height change is likely to explain the increase in the Seebeck

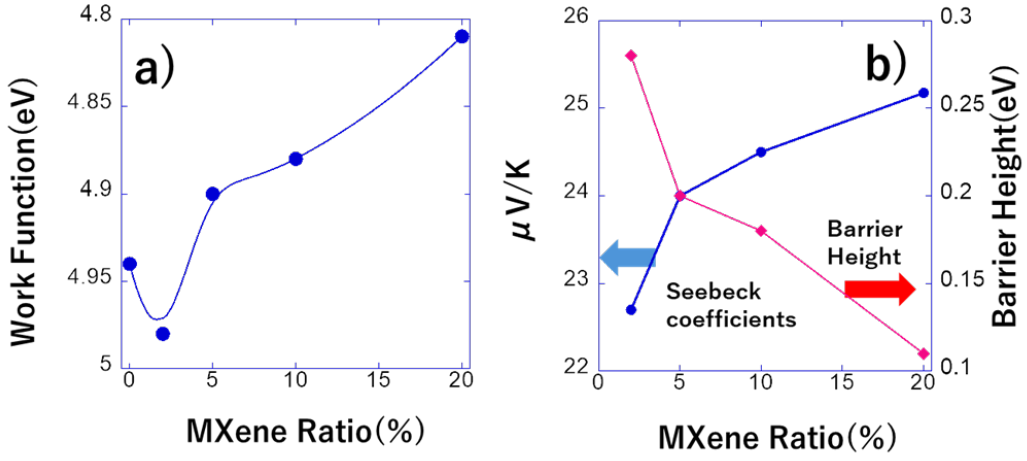

Fig. 5 (a)Work functions of PEDOT/PSS and hybrid films mixed with cleaved MXene with different MXene ratios; (b) Estimated energy barrier height and Seebeck coefficients of hybrid films mixed with cleaved MXene with different MXene ratios.

coefficients of hybrid films with cleaved MXene. However, in PEDOT/PSS with un-cleaved MXene, the changes in the work function and the apparent energy barrier height exhibit the same trend as those with cleaved MXene, but do not correspond to the increase in the Seebeck coefficient (Fig. S3). It is clear that when the MXene is large, the number of junctions contained in the film decreases. This difference can be explained quantitatively by assuming a function corresponding to the number of junctions. In contrast, in the case of PEDOT/PSS with MXene without cleavage, the change in the Seebeck coefficient is also within the range of experimental error, so it is thought to be almost constant. Whatever the case, we would like to consider the details of this phenomenon further using computational science and other methods.

On the other hand, the Seebeck coefficient improvement with cleaved MXene doping seen in the present data was not as great as that obtained by Guan and co-workers.[15] In the case of Guan *et al.*, the amount of MXene mixed in is very high compared with our film, so the Seebeck coefficient might be even higher. It is also possible that the Seebeck coefficient increases due to the contact potential with the metal electrode, because it has been suggested by several researchers that the Seebeck coefficient increases when metal electrodes are formed on the film.[38,39] Since no metal electrodes were formed on any of the films examined in the present study, we consider that Seebeck coefficient we obtained

might have been smaller than those measured by other researchers.

3-3. In-plane thermal conductivities and estimation of in-plane *zT*.

Thermal data of hybrid films with MXene for each ratio at 298 K are shown in Table 1. The in-plane thermal diffusivity decreases as the amount of MXene increases, whether or not cleavage is performed, except for 5% hybrid film with cleaved MXene. The specific heat decreases up to 10%, but actually increases at a MXene ratio of 20%. On the other hand, the measured density values in this study are slightly lower than the previously reported values (at around 1~1.5g/cm^3,[40,41]). Our results show that the value for PEDOT/PSS alone is around 1.0 g/cm^3, and even when MXene is added, it is still low, at around 1.4 g/cm^3. However, in actual PEDOT/PSS, not only are the crystalline and amorphous parts mixed together, but there are also differences depending on the fabrication method, and SEM and AFM photos of PEDOT/PSS after rinse treatment show that it is basically porous.[42,43] It is easy to imagine that a porous structure would show a density of less than 1.5 g/cm.^{3}

The thermal conductivity in the in-plane direction for cleaved MXene doped hybrid films tended not to decrease at a lower MXene ratio (cf. Table 1 and Fig. 6). However, at 20%, in-plane thermal conductivity further decreased to 0.9 W/mK. The thermal

conductivities of PEDOT/PSS film with un-cleaved MXene were also calculated for comparison. The thermal diffusivities were either slightly lower or almost the same as

Sample type	α // (m^2/s)	α ⊥ (m^2/s)	Cp (J/gK)	Density (g/cm^3)	k // (W/mK)	k ⊥ (W/mK)	Anisotropic Ratio of k
PEDOT/PSS	$9.21x10^{-7}$	$2.27 x10^{-7}$	1.75	1.02	1.44	0.41	3.54
13h 2%	$8.03x10^{-7}$	$1.55x10^{-7}$	1.67	0.95	1.31	0.25	5.32
13h 5%	$8.72 x10^{-7}$	$1.64 x10^{-7}$	1.60	1.10	1.38	0.29	4.80
13h 10%	$6.57 x10^{-7}$	$1.83 x10^{-7}$	1.46	1.33	1.25	0.36	3.50
13h 20%	$3.72 x10^{-7}$	$1.60 x10^{-7}$	1.71	1.41	0.90	0.39	2.33
0h 2%	$7.98x10^{-7}$	$1.78x10^{-7}$	1.83	0.96	1.40	0.31	4.49
0h 5%	$7.50 x10^{-7}$	$1.50x10^{-7}$	1.76	1.07	1.33	0.28	4.68
0h 10%	$6.35 x10^{-7}$	$1.51 x10^{-7}$	1.54	1.25	1.21	0.29	4.21
0h 20%	$5.49 x10^{-7}$	$1.50 x10^{-7}$	1.76	1.35	1.3	0.36	3.64

Table 2. Summary of the in-plane and through-plane thermal diffusivity, density, heat capacity, calculated in-plane and through-plane thermal conductivity and anisotropic ratios of PEDOT/PSS, and MXene/PEDOT/PSS hybrid films.

those of cleaved MXene/PEDOT/PSS hybrid films, with the result that reducing the size of MXene flakes is not so effective in decreasing the thermal conductivity at MXene ratios of less than 10%. We consider that as the ratio of the cleaved MXene increases, the flakes become smaller, and the dispersion in the film becomes more uniform, which has a significant effect on preventing heat conduction.

In the hybrid films with cleaved MXene, the trends in the changes in both the electrical and thermal conductivities were similar. Conversely, in the hybrid films with un-cleaved MXene, the trends in the changes in electrical conductivity and thermal conductivity were slightly different, *i.e.*, even at a ratio of 20%, the thermal conductivity did not decrease significantly. The difference is also thought to be related to the fact that the number of barriers to carrier movement in the films increases when the cleaved MXene is well dispersed at a higher ratio.

For comparison, the through-plane thermal diffusivities were also measured using aiPhase, and the obtained values were between 1.3 and $2.2 \times 10^{-7} m^2/s$, although there was no strong dependence on the ratios of MXene in hybrid films. The estimated through-plane thermal conductivities were in the 0.25 to 0.41 W/mK range. The ratio of the thermal conductivity in the through-plane and in-plane directions varied greatly, from 2.33 to 5.32, because the thermal conductivity in the in-plane decreased at a higher rate as the amount of MXene increased in the cleaved MXene.

Based on these thermal data, the in-plane *zT* values were calculated at a temperature of 298 K using the *PF* values at each MXene concentration (Fig. 6 and Table S4). Due to the decrease in thermal conductivity, the in-plane *zT* calculated using the maximum *PF* of the cleaved MXene/PEDOT/PSS film with DMSO rinsing at 5% undertaken twice is

0.019, which is much larger than that of PEDOT/PSS film without MXene (best *zT*, 0.01 as shown in Table S4). On the other hand, if we use the through-plane thermal conductivity and the highest *PF* at 5% cleaved MXene doped film with DMSO rinsing using the previous estimation method, the apparent *zT* is estimated to be 0.09, but it is only a reference. The in-plane *zT* values of hybrid films with un-cleaved MXene are lower than those of a sample doped with cleaved MXene, except for the 2% ratio sample (Fig. 6). The in-plane *zT* values of hybrid films with un-cleaved MXene are in the 0.008~0.01 range estimated using the average *PF*.

Let us compare the in-plane TE properties with those of other organic TE materials. It is said that if we are aiming to realize a practical device, we need to aim for *zT*~1.[44] However, polymers and new carbon TE materials are still far from reaching zT~1. For CNT, there are a few reports related to in-plane *zT* estimation. Horike *et al.*, reported that the in-plane thermal conductivity is estimated to be 38 W/mK for SWCNT films,[45] which is higher considerably in systems where *PF* exceeds 100 μW/mK^2, due to the high electrical conductivity of SWCNT thin film. They estimated the in-plane *zT* to be of the order of the 10^{-3}~10^{-4} in SWCNT film.[45] Matsumoto and colleagues are also working to reduce the anisotropy between the through and in-plane thermal conductivities by mixing polystyrene (PS) spheres into the SWCNT film.[46] When no PS spheres are added, the in-

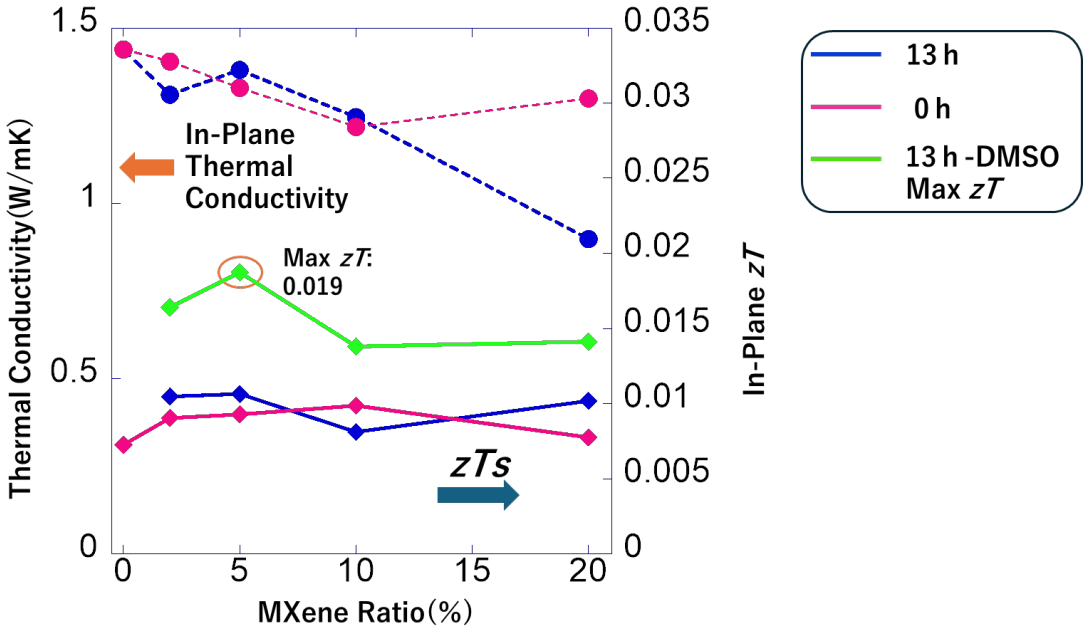

Fig. 6 Summary graph of in-plane thermal conductivities and in-plane *zT* values of MXene/PEDOT/PSS hybrid films and PEDOT/PSS films. The blue and red data correspond to 13h cleaved MXene doped and untreated MXene doped samples, respectively. The green data correspond to maximum in-plane *zT* 13h cleaved MXene doped hybrid films.

plane thermal conductivity is as high as 26 W/mK, and the *PF* exceeds 100 μW/mK^2, but the in-plane *zT* is of the order of 10^{-3}. In addition, although the in-plane thermal conductivity decreases to approximately 3 W/mK when PS is added, the *PF* also decreases to about 25μW/mK^2, so the in-plane *zT* does not change greatly. For CNT based

films, the in-plane *zT* did not increase because the higher in-plane thermal conductivity cancels out the effect of the increase in *PF* at that moment. With PEDOT/PSS thin film, for example, an electrical conductivity of 7000 S/cm has been reported to have a *PF* of 800 μW/mK^2 realized by a die coating technique, [8] however, since a high electrical conductivity also means a high thermal conductivity, it is thought that the in-plane *zT* will be small.

On the other hand, for PEDOT/PSS film with a *PF* of less than 50 μW/mK^2, we obtained an in-plane *zT* of the order of 10^{-2}, because the in-plane thermal conductivity is lower than that of an SWCNT film. Furthermore, the addition of a small amount of cleaved MXene effectively increased the Seebeck coefficient and further reduced the thermal conductivity, resulting in an increase in the in-plane *zT*. Thus, we believe that an approach that increases *PF and zT* by increasing the Seebeck coefficient while minimizing the in-plane thermal conductivity, is preferred for organic hybrid TE materials.

There have been reports of cases where the Seebeck coefficient is increased without increasing conductivity by processing PEDOT/PSS with strong acids and strong bases.[47,48] For example, with ultrathin PEDOT/PSS films treated with strong bases and acids, the Seebeck coefficient exceeds 60 μV/K, and a *PF* of 534.5 μW/mK^2 has been reported for a conductivity of around 1300 S/cm using PEDOT/PSS alone.[47] Even if we

assume a thermal conductivity of 1 W/mK in this case, the in-plane *zT* is still insufficient at around 0.15. If we aim for in-plane *zT*~1 at room temperature, we will need to take on the challenge of further increasing the Seebeck coefficient.

In conclusion, we have evaluated the TE properties of hybrid films of Ti-based MXene/PEDOT/PSS. The Seebeck coefficient increased for PEDOT/PSS with cleaved MXene. At a MXene ratio of 5% among the hybrid films, a maximum *PF* of 86.8 $\mu W/mK^2$ was obtained, by further rinsing with pure DMSO twice. In terms of changes in thermal conductivity, the effect of cleavage was hardly observed in except for films with 20% cleaved MXene, but the thermal conductivity was reduced overall. The thermal conductivity in the in-plane direction for cleaved MXene at 20% became 0.90 W/mK. At a MXene ratio of 5%, by rinsing with pure DMSO solvent, the in-plane *zT* reached its maximum at 0.019. Compared with CNT-based thin films, PEDOT/PSS doped with MXene has a high in-plane *zT* value, despite having a low *PF*, because of its low thermal conductivity. To obtain a high *zT* in the future, it is desirable to develop a method of obtaining a larger Seebeck coefficient without increasing thermal conductivity.

Author contributions

Investigation, T.I., MI.M., Writing – Original Draft, T.I.; Writing – Review& Editing,K.I.,MA.M., Supervision, K.I., A.Y. and M.O.

Conflict of interest

The authors declare that they have no known competing financial interests or personal relationships that could have appeared to influence the work reported in this paper.

Acknowledgements

We thank Dr. M. Nakano, Dr. Y. Kato, Dr. K. Yamamoto, Dr. Q. Wei and, Dr. M. Mukaida (AIST) for their experimental support and assistance with this work.

References

1. Q. Wei, M. Mukaida, K. Kirihara, Y. Naitoh, and T. Ishida *Materials,* 2015, **8**, 732-750.

2. B. Zhang, J. Sun, H. E. Katz, F. Fang, and R. L. Opila *ACS Appl.Mat.&Interface* 2010, **5**, 3170-3178.

3. G. H. Kim, L. Shao, K. Zhang, and K. P. Pipe, *Nat. Mater.* 2013, **12** 719-723.

4. Q. Wei, M. Mukaida, K. Kirihara, Y. Naitoh, and T. Ishida *Appl. Phys. Exp* 2014, **7.** 031601.

5. G.-H. Kim, J. Kim, and K. P. Pipe *Appl. Phys. Lett.* 2016, **108**, 093301.

6. E. J. Bae, Y. H. Kang, K.-S. Jang and S. Y. Cho *Sci Reports* 2016, **6**, 18805.

7. Z. Fan, D. Du, X. Guan, J. Ouyang, *Nano Energy* 2018, **51**, 481-488.

8. A. C. Hinckley, S. C. Andrews, M. T. Dunham, A. Sood, M. T. Barako, S. Schneider, M. F. Toney, K. E. Goodson, and Z. Bao *Adv. Electron. Mater.*2021, **7**, 2001190.

9. N. Toshima, and N. Jiravanichanun, *J.Electro Mat.* 2013, **42**,1882-1887.

10. L. Wang, Z. Zhang, Y., Liu B. Wang, L. Fang, J. Qiu, K. Zhang and S. Wang *Nat. Commun.* 2018, **9**, 3817.

11. H. Liu, P. Liu, M. Zhang, Z. Tian, N. Wang, Y. Liu and X. Zhang, *RSC Adv.* 2020, **10**, 33965-33971.

12.L. Zhang, Y. Harima, I. Imae, *Org. Electron.* 2017,51, 304–307.

13. X. Cao, M. Zhang, Y. Yang, H. Deng and Q. Fu, *Compos. Commun.* 2021,**27**,100869.

14. L. Zhang, B. Xia, X.-L. Shi, W.-D. Liu, Y. Yang, X. Hou, X. Ye, G. Suo and Z.-G. Chen, *Carbon* 2022,**196**, 718.

15. X. Guan, W. Feng, X. Wang R. Venkatesh and J. Ouyang *ACS Appl. Mater. Interfaces* 2020,**12**, 13013-13020.

16. J. Park, Y. Ko, J. Jeong, J. H. Song, J. S. Park and J. Kwak,*Mater. Res. Express.,* 2023, **10**, 055504.

17. B. Zhang, P. W. Wong, J. Guo, Y. Zhou, Y. Wang, J. Sun, M. Jiang, Z. Wang and A. K. An, *Nat. Commun.* 2022,**13**,3315.

18. J. Zhang, N. Kong, S. Uzun, A. Levitt, S. Seyedin, P. A. Lynch, S. Qin, M. Han, W. Yang, J. Liu, X. Wang, Y. Gogotsi, and J. M. Razal *Adv. Mat.* 2020, **32**, 2001093.

19. Z. Ling, C. E Ren, M-Q. Zhao, J. Yang, J. M. Giammarco, J. Qiu, M. W. Barsoum, Y. Gogotsi *Proc. Natl. Acad. Sci. U.S.A.* 2014,**111**,16676-16681.

20. S. Wustoni, A. Saleh, J. K. El-Demellawi, K. A. Hama, V. Druet, N. Wehbe, Y. Zhang and S. Inal, *APL Mater.* 2020,**8**, 121105.

21. G.Y. Yang, S.Z. Wang, H.T. Sun, X.M. Yao, C.B. Li, Y.J. Li and J.J Jiang *ACS Appl. Mater. Interfaces* 2021, 13, 57521-57531.

22. Z. Lin, H. Dang, C. Zhao, Y. Du, C. Chi, W. Ma, Y. Li and X. Zhang *Nanoscale*, 2022, **14**, 9419-9430.

23. M. He, J. Ge, Z. Q. Lin, X. H. Feng, X. W. Wang, H. B. Lu, Y. L. Yang and F. Qiu, *Energy Environ. Sci.*, 2012, **5**, 8351–8358.

24. C. Kim, J. Y. Baek, D. H. Lopez, D. H. Kim and H. Kim, *Appl. Phys. Lett.*, 2018, **113**, 153901.

25. Q. Wei, M. Mukaida, K. Kirihara, Y. Naitoh, and T. Ishida *RSC Adv.* 2014,**4**,28802-28806.

26. M. Mukaida, Q. Wei and T. Ishida *Synth. Met.* 2016, **225**, 64-69.

27. M. Mukaida, K. Kirihara and Q. Wei *ACS Appl. Ener. Mater.* 2019, **2**, 6973-6978.

28. R. Liu and W. Li, *ACS Omega*, 2018,**3**, 2609–2617.

29. R. Kang, Z. Zhang, L. Guo, J. Cui, Y. Chen, X. Hou, B. Wang, C.-T. Lin, N. Jiang and J. Yu, *Sci. Rep.* 2019,**9**, 9135.

30. J. Liu, X. Wang, D. Li, N.E. Coates, R.A. Segalman, D.G. Cahill *Macromol.* 2015, **48**, 585-591.

31. Q. Wei, M. Mukaida, K. Kirihara and T. Ishida *ACS Macro Lett.* 2014,**3**, 948-952.

32. R. Kato, A. Maesono and R. P. Tye *Int. J. Thermophys*. 2001,**22**, 617-629.

33. C. Gayner and Y. Amouyal *Adv. Funct. Mater.* 2020, **30**, 1901789.

34. Y. Wang, L. Yang, X.-L. Shi, X. Shi, L. Chen, M.S. Dargusch, J. Zou, Z.G. Chen, *Adv. Mater.* 2019,**31**, 1807916.

35.Y. Wang, X. Yang, A.G. Pandolfo, J. Ding, D. Li, *Adv. Energy Mater.* 2016, **6**, 1600185.

36. T. Schultz, J. Niederhausen, R. Schlesinger, S. Sadofev, and N. Koch, *J. Appl. Phys.* 2018,**123**, 245501.

37. S. Guo, S. K. Mohapatra, A. Romanov, T. V. Timofeeva, K. I. Hardcastle, K. Yesudas, C. Risko, J. L. Brédas, S. R. Marder, and S. Barlow, *Chem. Eur. J.* 2012,**18**, 14760-14772.

38. S. van Reenen and M. Kemerink *Org. Electron.*2014,**15**, 2250-2255.

39. I. Petsagkourakis, S. Riera-Galindo, T.-P. Ruoko, X. Strakosas, E. Pavlopoulou, X. Liu,S. Braun, R. Kroon, N. Kim, S. Lienemann, V. Gueskine, G. Hadziioannou, M. Berggren, M. Fahlman, S. Fabiano, K. Tybrandt, and X. Crispin, *Adv. Sci.,* 2023,**10**, 2206954.

40. D. M. DeLongchamp, B. D. Vogt, C. M. Brooks, K. Kano, J. Obrzut, C. A. Richter, O. A. Kirillov E. K. Lin, *Langmuir* 2005, **21**, 11480–11483.

41. A. Lenz, H. Kariis, A. Pohl, P. Persson and L. Ojamae *Chem. Phys.2011,* **384** 44-51.

42. D. A. Mengistie, P.-C. Wang and C.-W. Chu *J. Mater. Chem. A*, 2013, 1, 9907-9915.

43. C. S. Pathak, J. P. Singh and R. Singh, *Cur. Appl. Phys.*2014,**15**,528-534.

44. D.M. Rowe, *Renew. Energy* 1999,**16** ,1251-1256.

45. S. Horike, Q. Wei, K. Akaike, K. Kirihara, M. Mukaida, Y. Koshiba and K. Ishida *Nat. Comm.*2022, **13**, 3517.

46. M. Matsumoto, K. Shima, R. Yamaguchi, M. Mukaida M. Tomita, T. Ishida, T. Watanabe, T. Fujigaya, *STAM, 2021,* **22**, 272-279.

47. J. Park, J. G. Jang, K. Kang, S. H. Kim, and J. Kwak *Adv. Sci.* 2024, **11**, 2308368.

48. C. Li, D. Luo, T. Wang, C. Shan, C. Li, K. Sun, A. K. K. Kyaw, and J. Ouyang, *Small Struct.* 2023, **4**, 2300245.